JVI Journals.ASM.org

# Isolation and Characterization of a Novel *Betacoronavirus* Subgroup A Coronavirus, Rabbit Coronavirus HKU14, from Domestic Rabbits

**Susanna K. P. Lau,[a,b,c,d] Patrick C. Y. Woo,[a,b,c,d] Cyril C. Y. Yip,[d] Rachel Y. Y. Fan,[d] Yi Huang,[d] Ming Wang,[e] Rongtong Guo,[e] Carol S. F. Lam,[d] Alan K. L. Tsang,[d] Kenneth K. Y. Lai,[d] Kwok-Hung Chan,[d] Xiao-Yan Che,[f] Bo-Jian Zheng,[a,b,c,d] and Kwok-Yung Yuen[a,b,c,d]**

State Key Laboratory of Emerging Infectious Diseases,[a] Research Centre of Infection and Immunology,[b] Carol Yu Centre for Infection,[c] and Department of Microbiology,[d] The University of Hong Kong, Hong Kong, and Guangzhou Center for Disease Control and Prevention,[e] and Center of Laboratory, Zhujiang Hospital, Southern Medical University,[f] Guangzhou, China

**We describe the isolation and characterization of a novel *Betacoronavirus* subgroup A coronavirus, rabbit coronavirus HKU14 (RbCoV HKU14), from domestic rabbits. The virus was detected in 11 (8.1%) of 136 rabbit fecal samples by reverse transcriptase PCR (RT-PCR), with a viral load of up to $10^8$ copies/ml. RbCoV HKU14 was able to replicate in HRT-18G and RK13 cells with cytopathic effects. Northern blotting confirmed the production of subgenomic mRNAs coding for the HE, S, NS5a, E, M, and N proteins. Subgenomic mRNA analysis revealed a transcription regulatory sequence, 5′-UCUAAAC-3′. Phylogenetic analysis showed that RbCoV HKU14 formed a distinct branch among *Betacoronavirus* subgroup A coronaviruses, being most closely related to but separate from the species *Betacoronavirus 1*. A comparison of the conserved replicase domains showed that RbCoV HKU14 possessed <90% amino acid identities to most members of *Betacoronavirus 1* in ADP-ribose 1″-phosphatase (ADRP) and nidoviral uridylate-specific endoribonuclease (NendoU), indicating that RbCoV HKU14 should represent a separate species. RbCoV HKU14 also possessed genomic features distinct from those of other *Betacoronavirus* subgroup A coronaviruses, including a unique NS2a region with a variable number of small open reading frames (ORFs). Recombination analysis revealed possible recombination events during the evolution of RbCoV HKU14 and members of *Betacoronavirus 1*, which may have occurred during cross-species transmission. Molecular clock analysis using RNA-dependent RNA polymerase (RdRp) genes dated the most recent common ancestor of RbCoV HKU14 to around 2002, suggesting that this virus has emerged relatively recently. Antibody against RbCoV was detected in 20 (67%) of 30 rabbit sera tested by an N-protein-based Western blot assay, whereas neutralizing antibody was detected in 1 of these 20 rabbits.**

Coronaviruses (CoVs) are found in a wide variety of animals, in which they can cause respiratory, enteric, hepatic, and neurological diseases of various severities. Based on genotypic and serological characterizations, CoVs were traditionally classified into three distinct groups (5, 25). Recently, the Coronavirus Study Group of the International Committee on Taxonomy of Viruses (ICTV) has revised the nomenclature and taxonomy to classify coronaviruses into three genera, *Alphacoronavirus*, *Betacoronavirus*, and *Gammacoronavirus*, replacing the traditional group 1, 2, and 3 CoVs (7). Historically, alphacoronaviruses and betacoronaviruses were found in mammals, while gammacoronaviruses were found in birds, although recent findings also suggested the presence of gammacoronaviruses in mammals (21, 37, 70). Novel CoVs, which represented a novel genus, *Deltacoronavirus*, have also been identified in birds and pigs (69, 70, 74). As a result of the unique mechanism of viral replication, CoVs have a high frequency of recombination, which, coupled with high mutation rates, may allow them to adapt to new hosts and ecological niches (17, 25, 32, 67).

The discovery of the severe acute respiratory syndrome (SARS) coronavirus (SARS-CoV) as the causative agent of the SARS epidemic and the identification of SARS-CoV-like viruses from palm civets and horseshoe bats in China have boosted interests in the discovery of novel CoVs in both humans and animals (15, 27, 29, 35, 36, 42, 46, 71). During the post-SARS era, two novel human CoVs, both associated with respiratory tract infections, have been discovered. Human coronavirus NL63 (HCoV NL63), an alphacoronavirus, was reported independently by two groups in the Netherlands in 2004 (12, 60), whereas human coronavirus HKU1 (HCoV HKU1), a betacoronavirus, was identified in patients from Hong Kong in 2005 (28, 68, 72). As for animal CoVs, a previously unknown diversity of CoVs was described for various bat species in China and subsequently in other countries (9, 13, 30, 32, 43, 57, 59, 64, 73). In addition, a number of novel CoVs have been identified in other animals (10, 16, 21, 37, 70, 77), suggesting that our understanding of the diversity and evolution of CoVs in animals is still far from complete (74).

Despite the identification of horseshoe bats in China as the natural reservoir of SARS-CoV-like viruses, it is still unknown if these animals are the direct origin of SARS-CoV in civet and human (27, 29, 35). In particular, the spike protein of SARS-related *Rhinolophus* bat coronavirus (SARSr-Rh-BatCoV) showed only ~80% amino acid identity to that of civet SARS-CoV, with significant differences from the receptor binding domain of SARS-CoV (29, 35, 44). Since bats are commonly found and served in wild-animal markets and restaurants in Guangdong, which often house

**Received** 1 December 2011 **Accepted** 23 February 2012
**Published ahead of print** 7 March 2012
Address correspondence to Kwok-Yung Yuen, kyyuen@hkucc.hku.hk.
S.K.P.L. and P.C.Y.W. contributed equally to the manuscript.
Supplemental material for this article may be found at http://jvi.asm.org/.

doi:10.1128/JVI.06927-11

a variety of animals (65), we attempted to study other animals in Guangdong wet markets, which may have served as intermediate hosts for interspecies transmission or may harbor CoVs that could have recombined with SARSr-Rh-BatCoV to generate a SARS-CoV capable of infecting civet. During the investigations, a previously undescribed *Betacoronavirus* subgroup A CoV, rabbit coronavirus HKU14 (RbCoV HKU14), was detected in domestic rabbits. In this study, we describe the discovery and characterization of RbCoV HKU14, which was successfully isolated from HRT-18G and RK13 cell cultures. Complete genome analyses of four RbCoV HKU14 strains were carried out to study the genome features and molecular evolution in relation to those of other *Betacoronavirus* subgroup A CoVs. Subgenomic mRNA analysis and mapping of the transcription regulatory sequence (TRS) positions were performed by Northern blotting and determinations of the leader-body junction sequences.

## MATERIALS AND METHODS

**Sample collection.** All specimens were collected from live food animal markets in Guangzhou, China, from March 2006 to June 2009. A total of 165 animal or environmental samples from markets with a diversity of food animals and, subsequently, 136 fecal and 30 serum samples from domestic rabbits (*Oryctolagus cuniculus*) were collected by using procedures described previously (29, 70). All samples were placed into viral transport medium before transportation to the laboratory for nucleic acid extraction.

**RNA extraction.** Viral RNA was extracted from the samples by using a QIAamp viral RNA minikit (Qiagen, Hilden, Germany). The RNA was eluted in 60 μl of AVE buffer (Qiagen, Hilden, Germany) and was used as the template for reverse transcriptase PCR (RT-PCR).

**RT-PCR of the RdRp gene of CoVs using conserved primers and DNA sequencing.** Initial CoV screening was performed by amplifying a 440-bp fragment of the RNA-dependent RNA polymerase (RdRp) gene of CoVs using conserved primers (5′-GGTTGGGACTATCCTAAGTGTGA-3′ and 5′-CCATCATCAGATAGAATCATCATA-3′) designed by multiple alignments of the nucleotide sequences of available RdRp genes of known CoVs (29, 68). After the detection of the novel CoV RbCoV HKU14 from rabbit samples, subsequent screening was performed by amplifying a 320-bp fragment of the RdRp gene using the specific primers 5′-CGTATTGTTAGTAGTTTGGTA-3′ and 5′-ACAGTGTCACTTCTATACACA-3′. Reverse transcription was performed by using a SuperScript III kit (Invitrogen, San Diego, CA). The PCR mixture (25 μl) contained cDNA, PCR buffer (10 mM Tris-HCl [pH 8.3], 50 mM KCl, 2 mM $MgCl_2$, and 0.01% gelatin), 200 μM each deoxynucleoside triphosphate (dNTP) and 1.0 U *Taq* polymerase (Applied Biosystems, Foster City, CA). The mixtures were amplified with 60 cycles at 94°C for 1 min, 50°C for 1 min, and 72°C for 1 min and a final extension step at 72°C for 10 min in an automated thermal cycler (Applied Biosystems, Foster City, CA). Standard precautions were taken to avoid PCR contamination, and no false-positive result was observed for negative controls.

The PCR products were gel purified by using the QIAquick gel extraction kit (Qiagen, Hilden, Germany). Both strands of the PCR products were sequenced twice with an ABI Prism 3700 DNA analyzer (Applied Biosystems, Foster City, CA), using the two PCR primers. The sequences of the PCR products were compared with known sequences of RdRp genes of CoVs in the GenBank database.

**Viral culture.** Original fecal samples from two selected rabbits that tested positive for CoV by RT-PCR were subjected to virus isolation in Huh-7.5 (human hepatoma), Vero E6 (African green monkey kidney), HRT-18G (human rectum epithelial), RK13 (rabbit kidney), MDBK (bovine kidney), and BSC-1 (African green monkey renal epithelial) cells and specific-pathogen-free chicken embryos as described previously (34). Cell lines were prepared in culture tubes and inoculated with 200 μl of fecal samples diluted 1:10. Nonattached viruses were removed by washing the cells twice in phosphate-buffered saline. The monolayer cells were maintained in serum-free minimal essential medium (MEM; Invitrogen, NY), with or without supplementation by tosylsulfonyl phenylalanyl chloromethyl ketone (TPCK)-treated trypsin (1 μg/ml) (Sigma, St. Louis, MO). All infected cell lines were incubated at 37°C for 7 days. Cytopathic effects (CPE) were examined at days 1, 3, 5, and 7 by inverted light microscopy.

**Antigen detection by immunofluorescence.** Antigen detection of infected HRT-18G cell lines was performed by immunofluorescence (IF) according to protocols described previously (34). Cell smears at day 7 that were prepared and fixed in chilled acetone at −20°C for 10 min were tested with rabbit serum against RbCoV HKU14. The percentages of positive cells were recorded. An uninoculated cell smear was used as a negative control.

**Electron microscopy.** Negative-contrast electron microscopy was performed as described previously (24, 42). Tissue culture cell extracts infected with RbCoV HKU14 were centrifuged at 19,000 × *g* at 4°C, after which the pellet was resuspended in phosphate-buffered saline and stained with 2% phosphotungstic acid. Samples were examined with a Philips EM208s electron microscope.

**Real-time RT-PCR quantitation.** Real-time RT-PCR was performed on supernatants of infected cell lines and rabbit samples positive for RbCoV HKU14 by RT-PCR. Total nucleic acid was extracted from supernatants of infected cell lines at day 7, using EZ1 Advanced XL (Qiagen) as described previously (34). Reverse transcription was performed by use of the SuperScript III kit with random primers (Invitrogen, San Diego, CA). cDNA was amplified in a Lightcycler instrument with a FastStart DNA Master SYBR green I mix reagent kit (Roche Diagnostics GmbH, Germany) using specific primers (5′-GTGTGGTGGCTGTTATTATGTT-3′ and 5′-ACAGTGTCACTTCTATACACA-3′) targeting the RdRp gene of RbCoV HKU14, according to procedures described previously (26, 29). For quantitation, a reference standard was prepared by using the pCRII-TOPO vector (Invitrogen) containing the target sequence. Tenfold dilutions equivalent to 2 to $2 \times 10^7$ copies per reaction were prepared to generate concomitant calibration curves. At the end of the assay, PCR products (219-bp fragment of RdRp) were subjected to melting-curve analysis (65°C to 95°C, at 0.1°C/s) to confirm the specificity of the assay. The detection limit of this assay was 2 copies per reaction.

**Complete genome sequencing.** Four complete genomes of RbCoV HKU14 were amplified and sequenced using the RNA extracted from the original fecal specimens as templates. The RNA was converted to cDNA by a combined random-priming and oligo(dT)-priming strategy. The cDNA was amplified by degenerate primers designed by multiple alignments of the genomes of other CoVs with available complete genomes, using strategies described in our previous reports (29, 64, 68) and the CoV database CoVDB (19) for sequence retrieval. Additional primers were designed from the results of the first round and subsequent rounds of sequencing. These primer sequences are available upon request. The 5′ ends of the viral genomes were confirmed by the rapid amplification of cDNA ends using the 5′/3′ RACE kit (Roche, Germany). Sequences were assembled and manually edited to produce final sequences of the viral genomes.

**Genome analysis.** The nucleotide sequences of the genomes and the deduced amino acid sequences of the open reading frames (ORFs) were compared to those of other CoVs with complete genomes available by using the CoVDB database (19). The construction of phylogenetic trees was performed by the neighbor-joining method using ClustalX, with bootstrap values calculated from 1,000 trees. Protein family analysis was performed by the use of PFAM and InterProScan (3, 4). The prediction of transmembrane domains was performed by the use of TMpred and TMHMM (18, 54). Bootscan analysis was used to detect possible recombination, using a nucleotide alignment of the genome sequences of RbCoV HKU14 and related CoVs generated by ClustalX, version 2.1, and edited manually. Bootscan analysis was performed by using Simplot, version 3.5.1, as described previously (31, 32), with RbCoV HKU14 as the query.

**Estimation of divergence dates.** To allow a more accurate estimation of divergence time, the complete RdRp genes of a total of 10 RbCoV HKU14 strains (including the four strains with complete genome sequences) were sequenced. The divergence time was calculated based on RdRp gene sequence data using a Bayesian Markov chain Monte Carlo (MCMC) approach implemented in BEAST (version 1.6.1), as described previously (11, 27, 31, 55, 61, 62). One parametric model tree prior (constant size) and one nonparametric model tree prior (Bayesian skyline) were used for inference. Analyses were performed under the SRD06 model, using both a strict and a relaxed molecular clock. The MCMC run was $2 \times 10^8$ steps long, with sampling every 1,000 steps. Convergence was assessed on the basis of an effective sampling size after a 10% burn-in using Tracer software, version 1.5 (11). The mean time of the most recent common ancestor (tMRCA) and the highest-posterior-density regions at 95% (HPDs) were calculated, and the best-fitting models were selected by a Bayes factor using marginal likelihoods implemented in Tracer (55). A Bayesian skyline under a relaxed-clock model with an uncorrelated exponential distribution was adopted for making inferences, as Bayes factor analysis for the RdRp gene indicated that this model fitted the data better than the other models tested. The tree was summarized in a target tree by the Tree Annotator program included in the BEAST package by choosing the tree with the maximum sum of posterior probabilities (maximum clade credibility) after a 10% burn-in.

**Estimation of synonymous and nonsynonymous substitution rates.** The number of synonymous substitutions per synonymous site, $K_s$, and the number of nonsynonymous substitutions per nonsynonymous site, $K_a$, for each coding region among the four strains of RbCoV HKU14 were calculated by using Kumar in MEGA 4 (56).

**Northern blotting.** Total RNA was extracted from RbCoV HKU14-infected HRT-18G cells using TRIzol reagent (Invitrogen, Carlsbad, CA). RNA was separated on a 1% agarose gel with 7% formaldehyde at 100 V in 1× MOPS (morpholinepropanesulfonic acid) buffer (20 mM MOPS, 5 mM sodium acetate, 1 mM EDTA), transferred onto a positively charged nylon membrane (Amersham Biosciences, United Kingdom) with Transfer buffer (Ambion) by means of capillary force for 3 h, and cross-linked to the membrane with the chemical 1-ethyl-3-(3-dimethylaminopropyl) carbodiimide (Sigma-Aldrich, Germany) at 60°C for 1 h (40). The blot was prehybridized with ULTRAhyb-Oligo hybridization buffer (Ambion) and probed with an RbCoV HKU14 nucleocapsid-specific oligodeoxynucleotide probe, 5′-CCAGCACGATTTCCAGAGGACGCTCTACT-3′, which was labeled with digoxigenin (DIG) at the 3′ end. The blot was hybridized at 37°C overnight and washed with low- and high-stringency buffers as recommended by the manufacturer (Ambion). The detection of the DIG-labeled probe on the blot was performed by using a DIG Luminescent Detection kit according to the manufacturer's protocol (Roche, Germany).

**Determination of the leader-body junction sequence.** To determine the location of the leader and body TRSs used for RbCoV HKU14 mRNA synthesis, the leader-body junction sites and flanking sequences of all RbCoV HKU14 subgenomic mRNAs were determined by using RT-PCR as described previously (45, 77). Briefly, intracellular RNA was extracted from RbCoV HKU14-infected HRT-18G cells using TRIzol reagent (Invitrogen, Carlsbad, CA). Reverse transcription was performed by using random hexamers and the SuperScript III kit (Invitrogen, San Diego, CA). cDNA was PCR amplified with a forward primer located in the leader sequence and a reverse primer located in the body of each mRNA (see Table S1 in the supplemental material). The PCR mixture (25 μl) contained cDNA, PCR buffer (10 mM Tris-HCl [pH 8.3], 50 mM KCl, 2 mM $MgCl_2$, and 0.01% gelatin), 200 μM each dNTP, and 1.0 U *Taq* polymerase (Applied Biosystems, Foster City, CA). The mixtures were amplified for 40 cycles at 94°C for 1 min, 50°C for 1 min, and 72°C for 1 min and a final extension step at 72°C for 10 min in an automated thermal cycler (Applied Biosystems, Foster City, CA). RT-PCR products corresponding to each subgenomic mRNA could be distinguished by size differences upon agarose gel electrophoresis. PCR products were gel purified by using a QIAquick gel extraction kit (Qiagen, Hilden, Germany) and sequenced to obtain the leader-body junction sequences for each subgenomic mRNA.

**Cloning and purification of $His_6$-tagged recombinant RbCoV HKU14 nucleocapsid protein from *Escherichia coli*.** To produce fusion plasmids for protein purification, primers 5′-AACTCATATGATGTCCTTTACTCCTGGTAAGCA-3′ and 5′-GTTCCATATGTTATATTTCTGAGGTGTCTTCAG-3′ (for RbCoV HKU14) and primers 5′-CGGGATCCTCTTTTACTCCTGGTAAGCAATCC-3′ and 5′-GGGGTACCTTATATTTCTGAGGTGTCTTCAG-3′ (for human coronavirus OC43 [HCoV OC43]) were used to amplify the genes encoding the corresponding nucleocapsid proteins by RT-PCR as described previously (32, 66). The sequences coding for a total of 444 (RbCoV HKU14) and 453 (HCoV OC43) amino acid residues of the nucleocapsid proteins were amplified and cloned into the NdeI site of the pET-28b(+) expression vector (Novagen, Madison, WI) and the BamHI site and KpnI site of the pQE30 expression vector (Qiagen, Hilden, Germany) in frame and downstream of the series of six histidine residues, respectively. The $His_6$-tagged recombinant nucleocapsid proteins were expressed and purified by using the $Ni^{2+}$-loaded HiTrap chelating system (GE Healthcare, Buckinghamshire, United Kingdom) according to the manufacturer's instructions.

**Western blot analysis.** To detect the presence of antibodies against the RbCoV HKU14 N protein in rabbit sera and to test for possible cross-antigenicity between RbCoV HKU14 and HCoV OC43, 600 ng of purified $His_6$-tagged recombinant N protein of RbCoV HKU14 or HCoV OC43 was loaded into each well of a sodium dodecyl sulfate (SDS)–10% polyacrylamide gel and subsequently electroblotted onto a nitrocellulose membrane (Bio-Rad, Hercules, CA). The blot was cut into strips, and the strips were incubated separately with 1:4,000 dilutions of sera collected from 30 rabbits with serum samples available and sera from a patient with HCoV OC43 infection, 32 healthy blood donors, and 33 SARS patients. Antigen-antibody interactions were detected with 1:4,000-diluted horseradish peroxidase-conjugated anti-rabbit IgG or anti-human IgG (Zymed) and the ECL fluorescence system (GE Healthcare, Buckinghamshire, United Kingdom) as described previously (68, 71).

**Neutralization assays.** Neutralization assays for RbCoV HKU14 were carried out according to previously described protocols, with modifications (15, 29). Rabbit or human sera were serially diluted 1:2 and then mixed with 100 50% tissue culture infective doses of RbCoV HKU14 isolate R44. Available sera from 30 rabbits and human sera from a patient with HCoV OC43 infection, 10 healthy blood donors, and 10 SARS patients were included. After incubation for 1 h at 37°C, the mixture was inoculated in duplicate onto 96-well plates of HRT-18G cell cultures. Results were recorded after 6 days of incubation at 37°C.

**Nucleotide sequence accession numbers.** The nucleotide sequences of the four genomes of RbCoV HKU14 have been deposited in the GenBank sequence database under accession no. JN874559 to JN874562.

## RESULTS

**Identification of a novel CoV from rabbits.** Of 165 various animal/environmental samples from markets, RT-PCR for a 440-bp fragment in the RdRp gene of CoVs was positive for a potentially novel CoV in two samples, both from domestic rabbits (one rabbit anal swab sample and one rabbit cage swab sample). Sequencing results suggested that the potential novel virus was most closely related to members of the species *Betacoronavirus 1*, which includes bovine coronavirus (BCoV), equine coronavirus (ECoV), porcine hemagglutinating encephalomyelitis virus (PHEV), and HCoV OC43, with ≤91.6% nucleotide identities. In view of these preliminary results, fecal samples from 136 domestic rabbits were subsequently collected. RT-PCR using specific primers for this novel virus, RbCoV HKU14, was positive for 11 (8.1%) of these 136 samples. Quantitative RT-PCR showed that the viral load in the positive samples ranged from $9 \times 10^3$ to $1 \times 10^8$ copies/ml.

**TABLE 1** Coding potential and predicted domains in different proteins of RbCoV HKU14-1

| ORF | Nucleotide positions (start–end) | No. of nucleotides | No. of amino acids | Frame(s) | Predicted domain(s) | Positions (aa) |
|---|---|---|---|---|---|---|
| ORF1ab | 209–21663 | 21,455 | 7,151 | +1, +2 | —[a] | |
| NS2a1 | 21673–21804 | 132 | 43 | +1 | | |
| NS2a2 | 21829–22020 | 192 | 63 | +1 | | |
| NS2a3 | 22126–22254 | 129 | 42 | +1 | | |
| NS2a4 | 22277–22492 | 216 | 71 | +2 | | |
| HE | 22504–23778 | 1,275 | 424 | +1 | Hemagglutinin domain | 128–266 |
| | | | | | Cleavage site | Between 1 and 18, with signal peptide probability of 0.781 |
| | | | | | Active site for neuraminate *O*-acetyl-esterase activity, FGDS[b] | 37–40 |
| S | 23793–27881 | 4,089 | 1,362 | +3 | Type I membrane glycoprotein | 15–1306, exposed on outside |
| | | | | | Transmembrane domain | 1307–1327 |
| | | | | | Cytoplasmic tail rich in cysteine residues | |
| | | | | | Cleavage site | Between 763 and 768 |
| | | | | | 2 heptad repeats | 990–1091 (HR1), 1258-1303 (HR2) |
| NS5a | 28178–28507 | 330 | 109 | +2 | | |
| E | 28494–28763 | 270 | 89 | +3 | 2 transmembrane domains | 14–36 and 41–61 |
| M | 28760–29452 | 693 | 230 | +2 | 3 transmembrane domains | 35–45, 57–77, and 81–101; N-terminal 24 aa exposed on outside, C-terminal 126-aa hydrophilic domain inside |
| N | 29462–30796 | 1,335 | 444 | +2 | | |

[a] Shown in Table 2.
[b] See reference 63.

**Viral culture.** Of the six cell lines inoculated with rabbit samples positive for RbCoV HKU14, viral replication was detected by RT-PCR in the supernatants of HRT-18G and RK13 cells at day 7, with a viral load of $8 \times 10^6$ copies/ml in HRT-18G cells in the presence of trypsin. A CPE, mainly in the form of rounded, fused, and granulated giant cells rapidly detaching from the monolayer, was also observed for infected HRT-18G cells 5 days after inoculation, which showed viral nucleocapsid expression by IF in 40% of cells. Electron microscopy of ultracentrifuged cell culture extracts from infected HRT-18G cells showed the presence of CoV-like particles around 70 to 90 nm in diameter with typical club-shaped surface projections. Only a minimal CPE with cell rounding was observed for infected RK13 cells. Chicken embryos did not support the growth of RbCoV HKU14.

**Genome organization and coding potential of RbCoV HKU14.** Complete genome sequence data for four strains of RbCoV HKU14 were obtained by the assembly of the sequences of RT-PCR products from the RNA extracted directly from the corresponding individual specimens. The sizes of the genomes of RbCoV HKU14 were 30,904 to 31,116 bases, with a G+C content of 38%. The genome organization is similar to that of other *Betacoronavirus* subgroup A CoVs, with the characteristic gene order 5′-replicase ORF1ab, hemagglutinin-esterase (HE), spike (S), envelope (E), membrane (M), nucleocapsid (N)-3′ (Table 1 and Fig. 1). Moreover, additional ORFs coding for nonstructural proteins, NS2a and NS5a, were found.

CoVs are characterized by a unique mechanism of discontinuous transcription with the synthesis of a nested set of subgenomic mRNAs (47, 48). To assess the number and sizes of RbCoV HKU14 subgenomic mRNA species, a Northern blot analysis with a probe specific to the nucleocapsid sequence was performed. At least six distinct RNA species were identified, with sizes corresponding to predicted subgenomic mRNAs of HE (~8,650 bp), S (~7,350 bp), NS5a (~3,030 bp), E (~2,790 bp), M (~2,380 bp), and N (~1,680 bp) (Fig. 2A).

By determining the leader-body junction sequences of subgenomic mRNAs from RbCoV HKU14-infected cell cultures, the subgenomic mRNA sequences were aligned to the leader sequence, which confirmed the core sequence of the TRS motifs as 5′-UCUAAAC-3′ (Fig. 2B), as in other *Betacoronavirus* subgroup

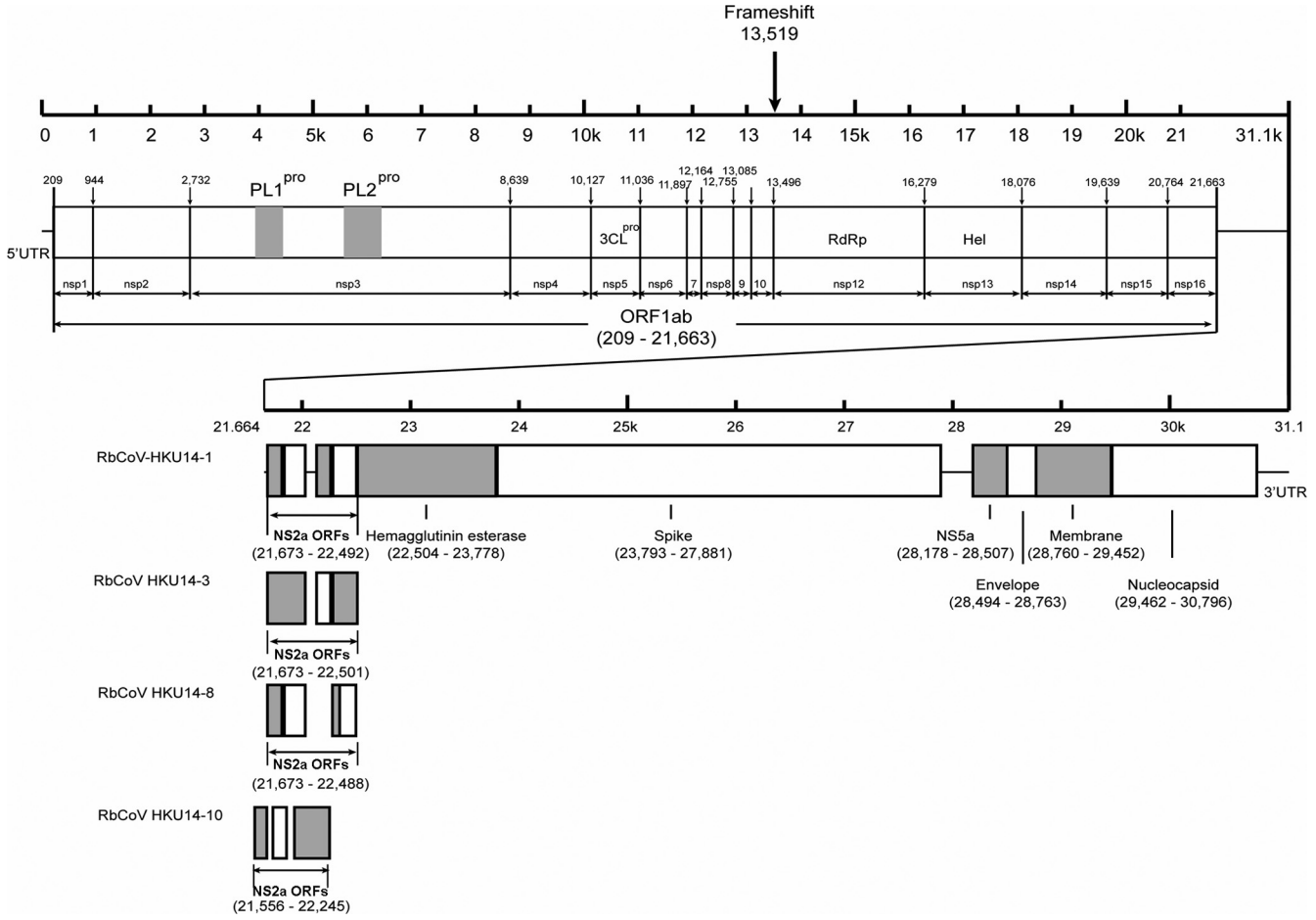


**FIG 1** Genome organization of RbCoV HKU14. Predicted ORFs, including ORF1ab, encoding the 16 nsp's and the NS2a, hemagglutinin-esterase, spike, NS5a, envelope, membrane, and nucleocapsid proteins are indicated with the corresponding nucleotide positions. The positions and arrangement of the small NS2a ORFs in the four strains of RbCoV HKU14 are shown in the expanded view. UTR, untranslated region.

A CoVs (20, 31, 75, 77). The leader TRSs and subgenomic mRNAs of HE, S, and N exactly matched each other, whereas there was a one-base mismatch for NS2a, NS5a, E, and M. The RbCoV HKU14 common leader on subgenomic mRNAs was confirmed as the first 63 nucleotides of the RbCoV HKU14 genome.

The coding potential and characteristics of putative nonstructural proteins (nsp's) of ORF1 of strain RbCoV HKU14-1 are shown in Tables 1 and 2, respectively. The ORF1 polyprotein possessed 72.0 to 87.2% amino acid identities to the polyproteins of other *Betacoronavirus* subgroup A CoVs. The predicted putative cleavage sites were conserved between RbCoV HKU14 and members of *Betacoronavirus 1* (Table 2). However, the lengths of nsp1, nsp2, nsp3, nsp13, and nsp15 in RbCoV HKU14 differed from those of corresponding nsp's in HCoV OC43, BCoV, ECoV, and/or PHEV, as a result of deletions or insertions. Interestingly, the genome of strain RbCoV HKU14-10 differed from the other three genomes in the nsp3 region by the presence of a 117-bp (39-amino-acid [aa]) deletion between PL2$^{pro}$ and the Y domain, which is a variable region among CoVs and carries an unknown function (79).

All *Betacoronavirus* subgroup A CoVs, except HCoV HKU1, possess an NS2a gene between ORF1ab and HE. Although the nucleotide sequence of RbCoV HKU14 at this region showed significant homology to that of the closely related species *Betacoronavirus 1*, RbCoV HKU14 is unique in having this region broken into several small ORFs. The number and size of these small ORFs vary among the four sequenced strains, with two strains having four and the other two strains having three small ORFs (Fig. 1 and 3). Nevertheless, analysis of the amino acid sequences of these small NS2a proteins showed that they possessed significant homologies to different regions of the single NS2a proteins in HCoV OC43, BCoV, ECoV, and PHEV (Fig. 3), and in between the small NS2a proteins of RbCoV HKU14 were deletions of amino acids conserved among the single NS2a proteins of HCoV OC43, BCoV, ECoV, and PHEV. Only two of these small NS2a proteins (NS2a4 of strain RbCoV HKU14-8 and NS2a3 of strain RbCoV HKU14-10) each contained one putative transmembrane domain predicted by TMHMM. Only the first small ORF, NS2a1, of RbCoV HKU14 was found to contain a preceding TRS, which was confirmed by the sequencing of its subgenomic mRNA leader-body junction (Fig. 2B). While the single NS2a proteins were highly conserved among members of *Betacoronavirus 1*, PHEV was found to possess a shorter single NS2a protein than HCoV OC43, BCoV, and ECoV as a result of the deletion of 84 amino acids at the C-terminal region (Fig. 3) (62). Although the *Betacoronavirus*-specific NS2 protein has been shown to be nonessential for *in vitro*

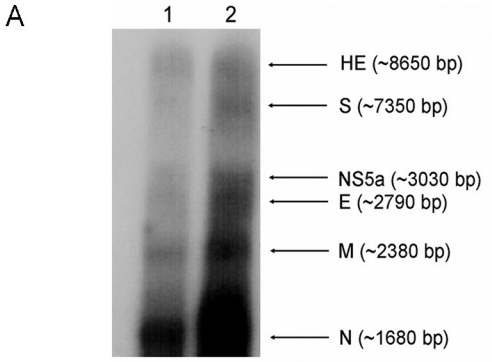


B

```
Leader       GUGCAUCCGCCUCAGUGAACUCUUGUUAGUUCUAAUUUAAUCUAAACUUUAUAAAAAC
mRNA (NS2a)  GUGCAUCCGCCUCAGUGAACUCUUGUUAGUUCUAAUUUAAUCUAAAUUUUAGAAAUG
genome          AAAGAAGUUUUUGUUGGUGAUAGUUUGGUUAAUGUAAUCUAAAUUUUAGAAAUG
                                                          *

Leader       GUGCAUCCGCCUCAGUGAACUCUUGUUAGUUCUAAUUUAAUCUAAACUUUAUAAAAAC
mRNA (HE)    GUGCAUCCGCCUCAGUGAACUCUUGUUAGUUCUAAUUUAAUCUAAACUCAGUGAAAAUG
genome          AAUUGUCUGAGGUUUUAUGAAUCUUCAUUUGAAGAAGACUAAACUCAGUGAAAAUG
                                                      *

Leader       GUGCAUCCGCCUCAGUGAACUCUUGUUAGUUCUAAUUUAAUCUAAACUUUAUAAAAAC
mRNA (S)     GUGCAUCCGCCUCAGUGAACUCUUGUUAGUUCUAAUUUAAUCUAAACAUG
genome          GAUAAUGGUACUAGGCUGCAUGAUGCUUAGACCAUAAUCUAAACAUG

Leader       GUGCAUCCGCCUCAGUGAACUCUUGUUAGUUCUAAUUUAAUCUAAACUUUAUAAAAAC
mRNA (NS5a)  GUGCAUCCGCCUCAGUGAACUCUUGUUAGUUCUAAUUUAAUCUAGACCUUAUAAC(40N)AUG
genome          CAGUAUUAGUACUAGUUCCAAACCAUAUUAUAAUUCGGGUAGACCUUAUAAC(40N)AUG
                                                      **  *

Leader       GUGCAUCCGCCUCAGUGAACUCUUGUUAGUUCUAAUUUAAUCUAAACUUUAUAAAAAC
mRNA (E)     GUGCAUCCGCCUCAGUGAACUCUUGUUAGUUCUAAUUUAAUCCAAACGUUAUGAU(115N)AUG
genome          AGGUAGCUUUUGUGCUACAUUUACUCUUUACGGCAAAUCCAAACGUUAUGAU(115N)AUG
                                                      *

Leader       GUGCAUCCGCCUCAGUGAACUCUUGUUAGUUCUAAUUUAAUCUAAACUUUAUAAAAAC
mRNA (M)     GUGCAUCCGCCUCAGUGAACUCUUGUUAGUUCUAAUUUAAUCCAAACAUUAUG
genome          GUAAAACCACCAGUCCUUGAUGUGGAUGACGUCUUAAUCCAAACAUUAUG
                                                      *

Leader       GUGCAUCCGCCUCAGUGAACUCUUGUUAGUUCUAAUUUAAUCUAAACUUUAUAAAAAC
mRNA (N)     GUGCAUCCGCCUCAGUGAACUCUUGUUAGUUCUAAUUUAAUCUAAACUUUAAGGAUG
genome          GGUUCUGGCAUGGACACCGCAUUGUUGAGAAAUAAUAUCUAAACUUUAAGGAUG
```

**FIG 2** (A) Northern blot analysis for total RNA isolated from RbCoV HKU14-infected HRT-18G cells. RNA species are indicated by arrows. HE, hemagglutinin; S, spike; NS5a, nonstructural NS5a; E, envelope; M, membrane; N, nucleocapsid. Lane 1, total RNA of 1 μg; lane 2, total RNA of 3 μg. (B) RbCoV HKU14 subgenomic mRNA leader-body junction and flanking sequences. The subgenomic mRNA sequences are shown in alignment with the leader and the genomic sequences. The start codon AUG in each subgenomic mRNA is depicted in boldface type. The putative TRS is underlined, and base mismatches between the body TRS and the leader TRS or the corresponding genomic region are indicated by asterisks. The 40N and 115N in parentheses indicate that 40 and 115 nucleotides at that region are not shown.

viral replication (50), cyclic phosphodiesterase domains in the NS2 proteins of coronaviruses as well as toroviruses have been predicted, and a possible role in viral pathogenicity in mouse hepatitis virus (MHV) was suggested (8, 53). Further studies are required to understand the potential function of NS2a proteins in different betacoronaviruses, including RbCoV HKU14.

The amino acid sequence of the predicted S protein of RbCoV HKU14 is most similar to that of BCoV, with 93.6 to 94.1% identities. A comparison of the amino acid sequences of the S proteins of RbCoV HKU14 and BCoV showed 64 amino acid polymorphisms, 13 of which were seen within the region previously identified as being hypervariable among the S proteins of other *Betacoronavirus* subgroup A CoVs (6, 16, 41) (Fig. 4), suggesting that this region in RbCoV HKU14 is also subject to strong immune selection. BCoV has been found to utilize *N*-acetyl-9-*O*-acetyl neuramic acid as a receptor for the initiation of infection (49). Among the five amino acids that may affect S1-mediated receptor binding in BCoV (78), three (threonine at position 11, asparagine at position 115, and methionine at position 118) were conserved in RbCoV HKU14 (Fig. 4). However, at positions 172 and 178, the asparagine and glutamine observed for BCoV were replaced by histidine and lysine in RbCoV, respectively. A previous study also identified seven amino acid substitutions in the S protein of BCoV that differed between virulent and avirulent cell culture-adapted

**TABLE 2** Characteristics of putative nonstructural proteins of ORF1 in RbCoV HKU14-1

| nsp | Putative function or domain(s)[a] | First amino acid residue[b] | Last amino acid residue[b] | Length (aa) | Length of corresponding protein in HCoV OC43, BCoV, ECoV, and PHEV (aa) |
|---|---|---|---|---|---|
| nsp1 | Leader protein | $M^{1}$ | $G^{245}$ | 245 | 246 (244 in ECoV) |
| nsp2 | MHV p65-like protein | $V^{246}$ | $A^{841}$ | 596 | 605 (601 in ECoV) |
| nsp3 | $PL1^{pro}$, $PL2^{pro}$, AC, ADRP, HD | $G^{842}$ | $G^{2810}$ | 1,969 | 1,899 (1,951 in ECoV) |
| nsp4 | HD | $A^{2811}$ | $Q^{3306}$ | 496 | 496 |
| nsp5 | $3CL^{pro}$ | $S^{3307}$ | $Q^{3609}$ | 303 | 303 |
| nsp6 | HD | $S^{3610}$ | $Q^{3896}$ | 287 | 287 |
| nsp7 | Unknown | $S^{3897}$ | $Q^{3985}$ | 89 | 89 |
| nsp8 | Unknown | $A^{3986}$ | $Q^{4182}$ | 197 | 197 |
| nsp9 | Unknown | $N^{4183}$ | $Q^{4292}$ | 110 | 110 |
| nsp10 | Unknown | $A^{4293}$ | $Q^{4429}$ | 137 | 137 |
| nsp11 | Unknown (short peptide at the end of ORF1a) | $S^{4430}$ | $V^{4443}$ | 14 | 14 |
| nsp12 | RdRp | $S^{4430}$ | $Q^{5357}$ | 928 | 928 |
| nsp13 | Hel | $S^{5358}$ | $Q^{5956}$ | 599 | 603 (599 in ECoV) |
| nsp14 | ExoN | $C^{5957}$ | $Q^{6477}$ | 521 | 521 |
| nsp15 | NendoU | $S^{6478}$ | $Q^{6852}$ | 375 | 375 (366 in ECoV and 374 in BCoV) |
| nsp16 | 2′-*O*-MT | $A^{6853}$ | $I^{7151}$ | 299 | 299 |

[a] $PL1^{Pro}$ and $PL2^{Pro}$, papain-like protease 1 and papain-like protease 2, respectively; AC, acidic domain; ADRP, ADP-ribose 1″-phosphatase; HD, hydrophobic domain; $3CL^{pro}$, 3C-like protease; RdRp, RNA-dependent RNA polymerase; Hel, helicase; ExoN, 3′-to-5′ exonuclease; NendoU, nidoviral uridylate-specific endoribonuclease; 2′-*O*-MT, ribose-2′-*O*-methyltransferase.

[b] Superscript numbers indicate positions.

strains (78). Interestingly, five of these seven "virulent" amino acids were also conserved in RbCoV, while amino acid substitutions were observed for the other two (valine to threonine at position 33 and aspartic acid to alanine at position 469). It was also reported previously that an amino acid change at position 531 of the S protein of BCoV discriminated between enteric (aspartic acid or asparagine) and respiratory (glycine) strains (76). In RbCoV HKU14, an aspartic acid was conserved at this site, which may be consistent with its detection in rabbit enteric samples.

Other predicted domains in the HE, S, NS5a, E, M, and N proteins of RbCoV HKU14-1 are summarized in Table 1. NS5a of RbCoV HKU14 is homologous to the corresponding nonstructural proteins of members of *Betacoronavirus 1*, with 85.3% to 91.7% amino acid identities. In MHV, the translation of the E protein is cap independent, via an internal ribosomal entry site (IRES) (58). However, a preceding TRS, 5′-UCCAAAC-3′, can be identified upstream of the E protein of RbCoV HKU14 (Fig. 2B), as in members of *Betacoronavirus 1* (77). Downstream of the N gene, the 3′-untranslated region contains a predicted bulged stem-loop structure of 64 nucleotides (nucleotide positions 30797 to 30860) conserved in betacoronaviruses (14). Downstream of this bulged stem-loop structure (nucleotide positions 30859 to 30910), a conserved pseudoknot structure, important for CoV replication, is also present.

**Phylogenetic analyses.** The phylogenetic trees constructed by using the amino acid sequences of the $3CL^{pro}$, RdRp, helicase (Hel), S, M, and N proteins of RbCoV HKU14 and other CoVs are shown in Fig. 5, and the corresponding pairwise amino acid identities are shown in Table 3. For all six genes, the four strains of RbCoV HKU14 formed a distinct cluster within *Betacoronavirus* subgroup A CoVs, and among the known *Betacoronavirus* subgroup A CoVs, they were more closely related to members of the species *Betacoronavirus 1*, BCoV, ECoV, PHEV, and HCoV OC43, than to MHV and HCoV HKU1. However, a comparison of the amino acid sequences of the seven conserved replicase domains (ADP-ribose 1″-phosphatase [ADRP], nsp5 [$3CL^{pro}$], nsp12 [RdRp], nsp13 [Hel], nsp14 [3′-to-5′ exonuclease {ExoN}], nsp15 [NendoU], and nsp16 [ribose-2′-*O*-methyltransferase {O-MT}]) for coronavirus species demarcation (7) showed that RbCoV HKU14 possessed <90% amino acid identities to members of *Betacoronavirus 1* in the ADRP (except ECoV) and NendoU domains (see Table S2 in the supplemental material), indicating that RbCoV HKU14 represented a separate species among members of *Betacoronavirus* subgroup A. Based on the present results, we propose a novel species, rabbit coronavirus HKU14 (RbCoV HKU14), to describe this virus under *Betacoronavirus* subgroup A CoVs.

**Recombination analyses.** Interestingly, changes in the phylogenetic position in relation to members of *Betacoronavirus 1* were observed among different regions of the RbCoV HKU14 genome (Fig. 5). For Hel, RbCoV HKU14 is most closely related to ECoV, with 98.8 to 99% amino acid identities, than to BCoV, PHEV, and HCoV OC43. As for S and N, it is more closely related to BCoV and HCoV OC43 than to ECoV and PHEV. This suggests that recombination may have occurred among these viruses during their evolution. Bootscan analysis detected potential recombination at various sites of the RbCoV HKU14 genome, most notably at around positions 7100 and 20350 (Fig. 6A).

Upstream of position 7100, RbCoV HKU14 exhibited high bootstrap support for clustering with ECoV, but an abrupt drop in clustering was observed downstream of position 7100. Similarity plot and sequence alignment analyses showed that upstream of position 7100, RbCoV HKU14 possessed a higher level of sequence similarity to ECoV than to PHEV, BCoV, and HCoV OC43, as a result of deletions in the latter three viruses (Fig. 6B, and see Fig. S1A in the supplemental material). However, such close similarity to ECoV was no longer observed downstream of position 7100. This suggested that RbCoV HKU14 and ECoV have

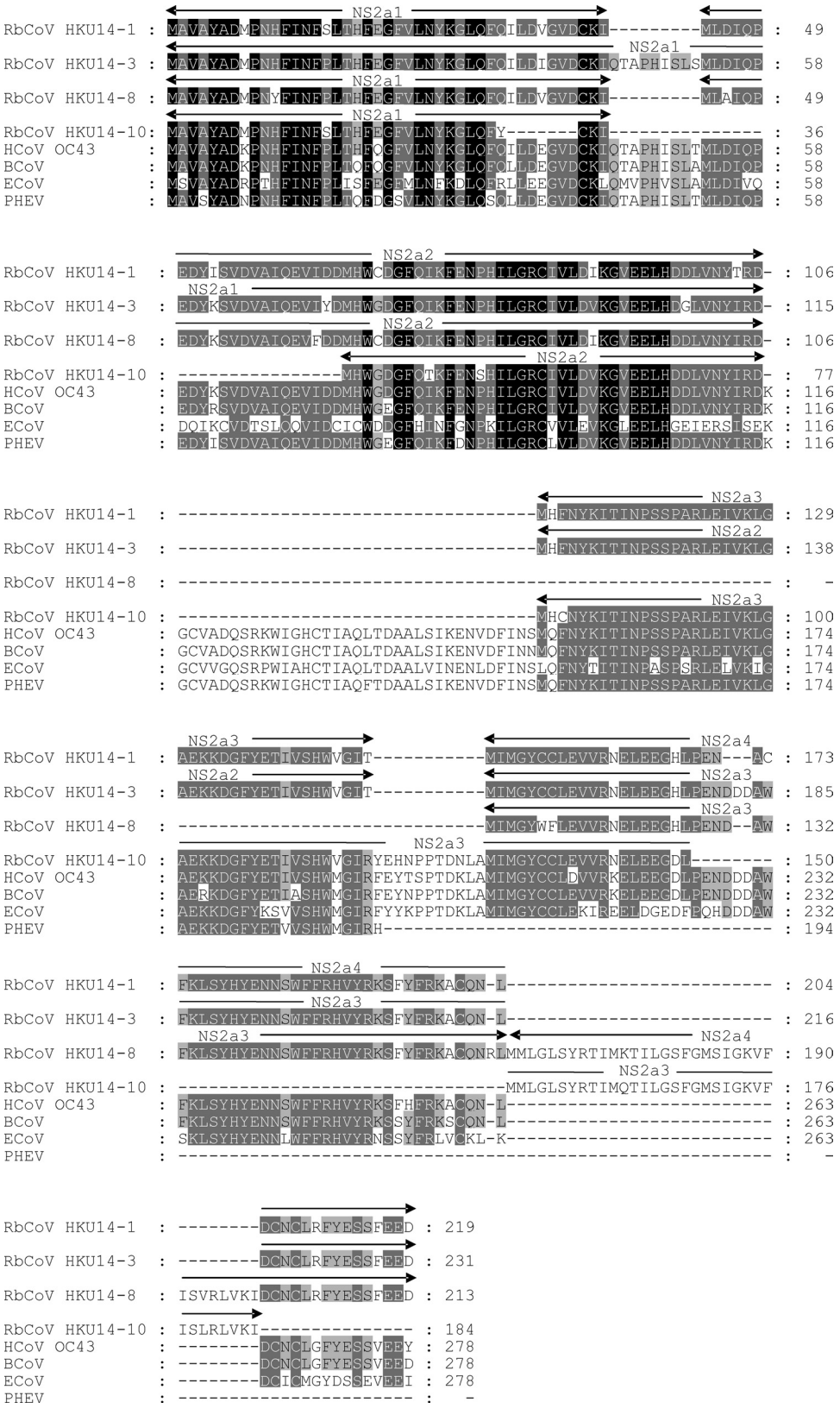


**FIG 3** Multiple alignment of predicted amino acid sequences of small NS2a proteins of RbCoV HKU14 compared to the single NS2a proteins of members of *Betacoronavirus 1*. The small NS2a proteins of RbCoV HKU14 are marked above the corresponding sequences. Identical and highly conserved amino acid residues among all viruses are highlighted in black and gray, respectively.

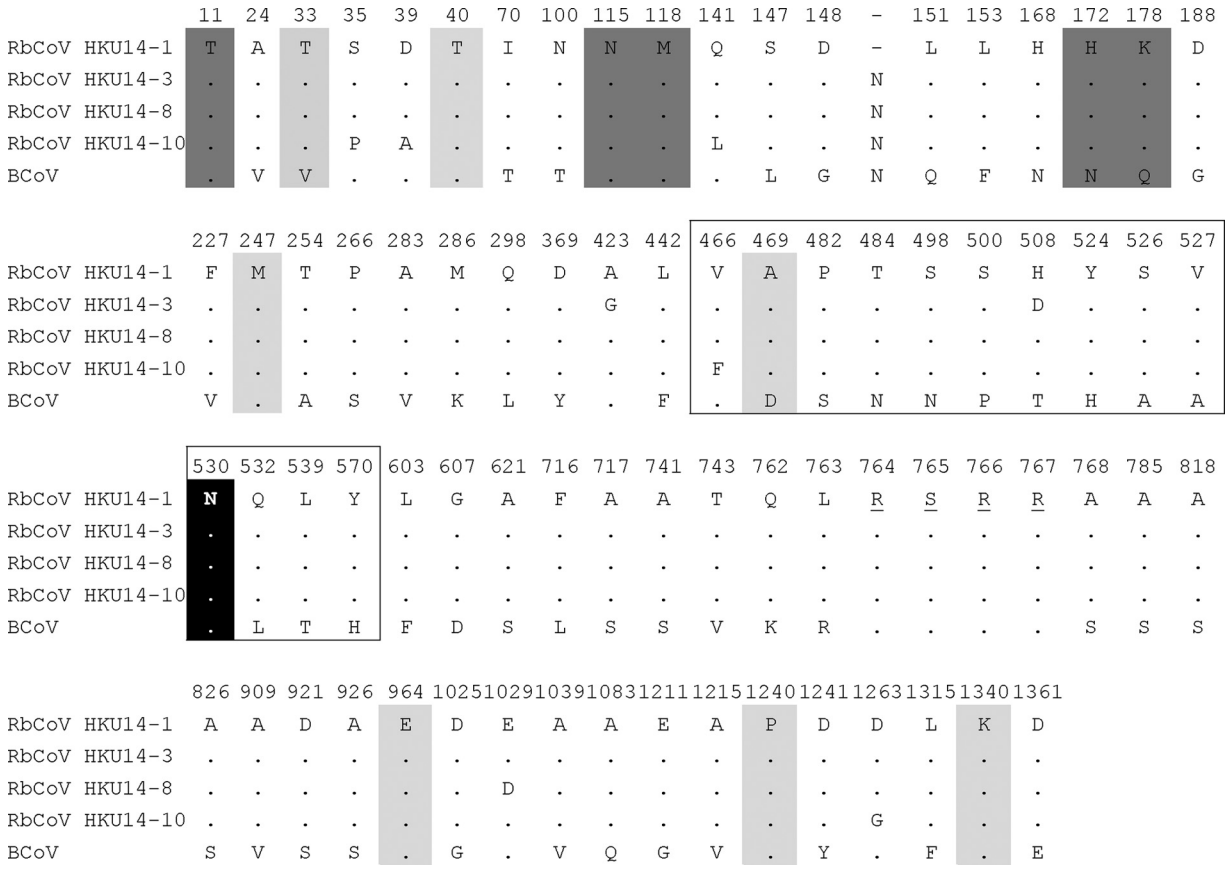


**FIG 4** Amino acid comparison of the S protein of RbCoV HKU14 to that of BCoV, showing sites of amino acid substitutions, amino acids important for virulence and receptor binding in BCoV, and sites of cleavage. Amino acid positions are given with reference to strain RbCoV HKU14-1 which possessed an amino acid deletion after residue 148, where an asparagine was present in other strains. Conserved amino acids compared to those of RbCoV HKU14-1 are represented by dots. Amino acids of putative cleavage sites are underlined. Amino acids within the S1 hypervariable region of BCoV are marked with open boxes. Amino acid sites important for virulence in BCoV are highlighted in light gray. Amino acid sites shown to affect S1-mediated receptor binding in BCoV are highlighted in dark gray. The amino acid site which discriminated between enteric and respiratory BCoV strains is highlighted in black.

probably coevolved at the region upstream of position 7100, although a recombination event could not be ascertained.

Upstream of another potential recombination site at position 20350, RbCoV HKU14 exhibited high bootstrap support for clustering with ECoV, but an abrupt drop in clustering was observed downstream of position 20350. Similarity plot and sequence alignment analyses showed that upstream of position 20350, RbCoV HKU14 possessed a higher level of sequence similarity to ECoV than to PHEV, BCoV, and HCoV OC43, whereas downstream of position 20350, RbCoV HKU14 possessed a higher level of sequence similarity to BCoV and HCoV OC43 than to ECoV and PHEV (Fig. 6B, and see Fig. S1B and S1C in the supplemental material). A phylogenetic analysis of partial sequences upstream and downstream of position 20350 also showed a shift of the phylogenetic clustering of RbCoV HKU14, which clustered with ECoV upstream (Fig. 6C) and with BCoV and HCoV OC43 downstream (Fig. 6D) of position 20350. These findings indicated that recombination may have taken place at around position 20350 (corresponding to nsp15) between ECoV and BCoV/HCoV OC43 in the generation of RbCoV HKU14.

**Estimation of divergence dates.** Using the uncorrelated relaxed-clock model on RdRp gene sequences, the date of tMRCA of RbCoV HKU14, BCoV, and HCoV OC43 was estimated to be 1846.25 (HPDs, 1673.18 to 1958.81), approximately 165 years ago (Fig. 7). The date of divergence between HCoV OC43 and BCoV was estimated to be 1929.71 (HPDs, 1881.95 to 1960.19), approximately 81 years ago. Moreover, the date of tMRCA of the 10 RbCoV HKU14 strains was estimated to be 2002.05 (HPDs, 1997.34 to 2005.01). The estimated mean substitution rate of the RdRp data set was $3.774 \times 10^{-4}$ substitutions per site per year, which is comparable to previous estimations for other *Betacoronavirus* subgroup A CoVs (31, 61, 62).

**Estimation of synonymous and nonsynonymous substitution rates.** The $K_a/K_s$ ratios for the various coding regions in RbCoV HKU14 are shown in Table S3 in the supplemental material. The $K_a/K_s$ ratios of most ORFs were low, suggesting that these ORFs were under purifying selection. The ORF with the highest $K_a/K_s$ ratio was ORF1ab, especially at nsp2.

**Serological studies.** Among tested sera from 30 rabbits with samples available, 20 (67%) were positive and 10 (33%) were negative for antibody against the recombinant RbCoV HKU14 N protein by Western blot assays. All positive sera were obtained from rabbits negative for RbCoV HKU14 by RT-PCR. Possible cross-antigenicity between the RbCoV HKU14 and HCoV OC43 N proteins was found. All rabbit serum samples positive for RbCoV HKU14 antibody were also positive by a Western blot assay based

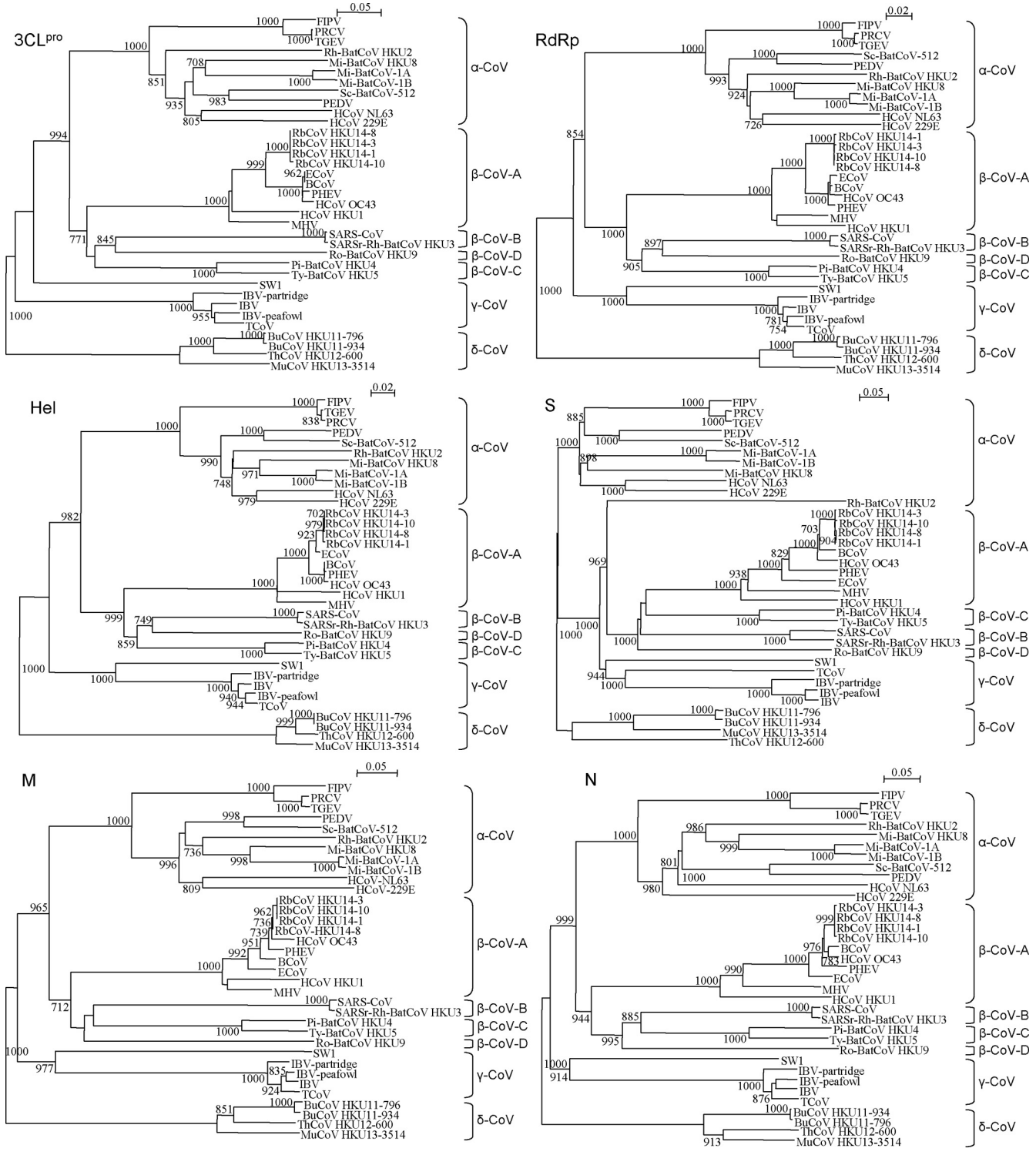


**FIG 5** Phylogenetic analyses of chymotrypsin-like protease (3CL$^{pro}$), RNA-dependent RNA polymerase (RdRp), helicase (Hel), spike (S), membrane (M), and nucleocapsid (N) of RbCoV HKU14. The trees were constructed by the neighbor-joining method using Kimura's two-parameter correction and bootstrap values calculated from 1,000 trees. A total of 318, 959, 609, 1,791, 303, and 609 amino acid positions in 3CL$^{pro}$, RdRp, Hel, S, M, and N, respectively, were included in the analyses. The scale bar indicates the estimated number of substitutions per 20 or 50 amino acids. HCoV 229E, human coronavirus 229E (GenBank accession no. NC_002645); PEDV, porcine epidemic diarrhea virus (accession no. NC_003436); TGEV, porcine transmissible gastroenteritis virus (accession no. NC_002306); FIPV, feline infectious peritonitis virus (accession no. AY994055); PRCV, porcine respiratory coronavirus (accession no. DQ811787); HCoV NL63, human coronavirus NL63 (accession no. NC_005831); Rh-BatCoV HKU2, *Rhinolophus* bat coronavirus HKU2 (accession no. EF203064); Ty-BatCoV HKU4, *Tylonycteris* bat coronavirus HKU4 (accession no. NC_009019); Pi-BatCoV HKU5, *Pipistrellus* bat coronavirus HKU5 (accession no. NC_009020); Mi-BatCoV-HKU8, *Miniopterus* bat coronavirus HKU8 (accession no. NC_010438); Ro-BatCoV HKU9, *Rousettus* bat coronavirus HKU9 (accession no. NC_009021), Mi-Bat-CoV-1A, *Miniopterus* bat coronavirus 1A (accession no. NC_010437); Mi-BatCoV-1B, *Miniopterus* bat coronavirus 1B (accession

on a recombinant HCoV OC43 N protein. Moreover, human sera from a patient with HCoV OC43 infection, 28 of 32 healthy blood donors, and 32 of 33 SARS patients were positive for antibody against a recombinant RbCoV HKU14 N protein by a Western blot assay. Neutralization assays for RbCoV HKU14 were therefore performed to detect neutralizing antibodies in rabbit and human sera. One of the 20 rabbit sera positive for antibody against the recombinant RbCoV HKU14 N protein and human sera from a patient with HCoV OC43 infection, 5 of 10 healthy blood donors, and 4 of 10 SARS patients were found to possess neutralizing antibody to RbCoV HKU14 with a titer of ≥1:8.

## DISCUSSION

We isolated and characterized a novel *Betacoronavirus* subgroup A CoV, RbCoV HKU14, from domestic rabbits in wet markets in Guangzhou, China. *Betacoronavirus* subgroup A CoVs include the traditional "group 2 CoVs," including MHV, HCoV HKU1, HCoV OC43, BCoV, and PHEV, whereas SARS-CoV-like viruses were classified under *Betacoronavirus* subgroup B CoVs. Bat CoVs belonging to two novel subgroups, subgroups C and D, were also recently identified, with genome features distinct from those of *Betacoronavirus* subgroup A and subgroup B CoVs (64). RbCoV HKU14 formed a distinct branch within *Betacoronavirus* subgroup A CoVs upon phylogenetic analysis, being most closely related to but separate from members of the species *Betacoronavirus 1*. Moreover, RbCoV HKU14 possessed <90% amino acid identities to members of *Betacoronavirus 1* in two (ADRP and NendoU) of the seven conserved replicase domains for coronavirus species demarcation by the ICTV (7). This supported that RbCoV HKU14 should represent a separate species among members of *Betacoronavirus* subgroup A, instead of another member of the species *Betacoronavirus 1*. In addition, RbCoV HKU14 possessed certain genomic features different from those of related *Betacoronavirus* subgroup A CoVs. As a result of deletions or insertions, the lengths of five of the nsp's in ORF1 were different from those of the corresponding nsp's in one or more members of *Betacoronavirus 1*. The NS2a region of RbCoV HKU14 is also unique among *Betacoronavirus* subgroup A CoVs, being broken into a variable number of small ORFs, with only the first ORF, NS2a1, containing a preceding TRS. Since unique CoV proteins may be involved in replication and virulence (38), further studies are warranted to understand the potential function of these small NS2a proteins in RbCoV HKU14. In this study, RbCoV HKU14 was detected in 8.1% of fecal samples among tested rabbits. A Western blot assay based on a recombinant RbCoV HKU14 N protein showed the presence of antibody in a high percentage of tested rabbit sera (67%), although neutralizing antibody to the virus was detected in only one rabbit. This may suggest that Western blot assays based on the coronavirus N protein alone may not be specific. Nevertheless, the high rate of detection of RbCoV HKU14 in fecal samples, together with the low $K_a/K_s$ ratios observed for most of its ORFs, including the S gene, suggested that rabbits are likely the natural reservoir of RbCoV HKU14. Interestingly, anti-RbCoV HKU14 N antibodies and neutralizing antibody to RbCoV HKU14 were also detected in a significant proportion of healthy blood donors and SARS patients. This may due to the presence of cross-reacting antibodies due to past infection by human betacoronaviruses such as HCoV OC43, in line with our previous findings on cross-reactivity between HCoV OC43 and SARS-CoV (66). Further studies are required to understand the cross-reactivity among the different betacoronaviruses.

RbCoV HKU14 is likely to be only distantly related to a rabbit CoV previously found to cause myocarditis in rabbits. The latter rabbit CoV, which originated from contaminated samples of *Treponema pallidum* used in a rabbit infection model at Johns Hopkins University, was detected by electron microscopy and found to cross-react with alphacoronaviruses, including human coronavirus 229E (HCoV 229E), feline infectious peritonitis virus, canine coronavirus diarrhea virus, and transmissible gastroenteritis virus, in serological assays (51). This virus was subsequently used as a model for virus-induced myocarditis and dilated cardiomyopathy (2). Although no gene sequence for this virus is available, the existing data suggested that it is an alphacoronavirus, and its host of origin still remains obscure.

The ability of RbCoV HKU14 to grow readily in human cell cultures, inducing cytopathic effects, is intriguing. With only a few exceptions, such as SARS-CoV, CoVs are notoriously difficult to culture in cell lines. HCoV OC43 and HCoV 229E, even if isolated, induce only subtle or nonexistent cytopathic effects. Despite being closely related to SARS-CoV, SARSr-Rh-BatCoV from horseshoe bats has not been isolated in cells susceptible to SARS-CoV. In the present study, RbCoV HKU14 was able to replicate in both rabbit kidney (RK13) and human rectum epithelial (HRT-18G) cells, with cell rounding and fusion to giant cells rapidly detaching from the monolayer in HRT-18G cells being observed after 5 days of inoculation. HCoV OC43, BCoV, ECoV, and the MHV-H2 variant are also known to replicate in HRT-18 cells, suggesting that these *Betacoronavirus* subgroup A CoVs may share similar cellular tropisms. All rabbits positive for RbCoV HKU14 in their fecal samples appeared healthy at the time of sampling. While CoVs are associated with a wide spectrum of diseases in animals, many CoVs, especially those from bats, were detected in apparently healthy individuals without evidence of overt disease (27, 29, 30, 32, 35, 57, 64). Interestingly, the aspartic acid within the S protein specific to enteric strains of BCoV was conserved in RbCoV HKU14, which may be compatible with its enteric tropism. Domestic rabbits are descended from the wild European or Old World rabbit, *Oryctolagus cuniculus*, originating from Southern Europe and North Africa (39). While China is one of the main producers of rabbit meat, farming of the species is increasing,

no. NC_010436); Sc-BatCoV-512, *Scotophilus* bat coronavirus 512 (accession no. NC_009657); HCoV HKU1, human coronavirus HKU1 (accession no. NC_006577), HCoV OC43, human coronavirus OC43 (accession no. NC_005147); MHV, mouse hepatitis virus (accession no. NC_006852); BCoV, bovine coronavirus (accession no. NC_003045); ECoV, equine coronavirus (accession no. NC_010327); PHEV, porcine hemagglutinating encephalomyelitis virus (accession no. NC_007732); SARS-CoV (human), human SARS coronavirus (accession no. NC_004718); SARSr-Rh-batCoV HKU3, SARS-related *Rhinolophus* bat coronavirus HKU3 (accession no. NC_009694); IBV, infectious bronchitis virus (accession no. NC_001451); IBV-partridge, partridge coronavirus (accession no. AY646283); IBV-peafowl, peafowl coronavirus (accession no. AY641576); TCoV, turkey coronavirus (accession no. NC_010800); SW1, beluga whale coronavirus (accession no. NC_010646); BuCoV HKU11-796, bulbul coronavirus HKU11-796 (accession no. NC_011548); BuCoV HKU11-934, bulbul coronavirus HKU11-934 (accession no. FJ376619); ThCoV HKU12-600, thrush coronavirus HKU12-600 (accession no. NC_011549); MunCoV HKU13-3514, munia coronavirus HKU13-3514 (accession no. NC_011550).

**TABLE 3** Comparison of genomic features of RbCoV HKU14 and other CoVs with complete genome sequences available and amino acid identities between the predicted 3CL$^{pro}$, RdRp, Hel, HE, S, M, and N proteins of RbCoV HKU14 and the corresponding proteins of other CoVs

| CoV[a] | Genome size (no. of bases) | G+C content | Pairwise amino acid identity (%) | | | | | | |
|---|---|---|---|---|---|---|---|---|---|
| | | | 3CL$^{pro}$ | RdRp | Hel | HE | S | M | N |
| *Alphacoronavirus* | | | | | | | | | |
| PEDV | 28,033 | 0.42 | 43.9 | 58.7 | 58.4 | | 25.5 | 38.2 | 22.9 |
| TGEV | 28,586 | 0.38 | 47.4 | 58.1 | 58.7 | | 26.3 | 35.2 | 27.5 |
| FIPV | 29,355 | 0.38 | 47.7 | 58.5 | 58.4 | | 25.8 | 33.1 | 26.5 |
| HCoV 229E | 27,317 | 0.38 | 44.2 | 55.9 | 57.4 | | 26.1 | 31.8 | 25.4 |
| HCoV NL63 | 27,553 | 0.34 | 43.1 | 56.0 | 57.6 | | 26.1 | 34.9 | 24.4 |
| Rh-BatCoV HKU2 | 27,165 | 0.39 | 44.9 | 57.5 | 55.6 | | 25.0 | 36.3 | 26.3 |
| Mi-BatCoV-1A | 28,326 | 0.38 | 42.9 | 58.0 | 57.6 | | 25.6 | 31.0 | 26.5 |
| Mi-BatCoV-1B | 28,476 | 0.39 | 42.6 | 57.3 | 57.6 | | 25.7 | 31.3 | 27.4 |
| Mi-BatCoV HKU8 | 28,773 | 0.42 | 44.2 | 58.3 | 55.4 | | 26.4 | 34.3 | 27.4 |
| Sc-BatCoV 512 | 28,203 | 0.40 | 43.4 | 58.2 | 57.7 | | 25.5 | 38.6 | 26.9 |
| *Betacoronavirus* subgroup A | | | | | | | | | |
| HCoV OC43 | 30,738 | 0.37 | 91.7 | 94.6 | 96.2 | 93.6 | 90.5 | 96.5 | 94.4 |
| BCoV | 31,028 | 0.37 | 92.7 | 95.5 | 96.4 | 96.2 | 94.1 | 95.7 | 94.6 |
| PHEV | 30,480 | 0.37 | 92.1 | 95.3 | 96.4 | 89.4 | 82.7 | 95.7 | 92.9 |
| ECoV | 30,992 | 0.37 | 92.7 | 95.0 | 98.8 | 72.4 | 81.2 | 91.7 | 91.7 |
| MHV | 31,357 | 0.42 | 86.8 | 91.1 | 91.2 | 58.1 | 64.1 | 85.3 | 71.5 |
| HCoV HKU1 | 29,926 | 0.32 | 85.8 | 89.0 | 89.7 | 53.5 | 64.2 | 77.8 | 66.1 |
| RbCoV HKU14-1 | 31,100 | 0.38 | | | | | | | |
| *Betacoronavirus* subgroup B | | | | | | | | | |
| SARS-CoV | 29,751 | 0.41 | 48.4 | 66.2 | 67.7 | | 31.1 | 38.7 | 34.3 |
| SARSr-Rh-BatCoV HKU3 | 29,728 | 0.41 | 48.0 | 66.1 | 68.2 | | 30.2 | 39.1 | 34.7 |
| *Betacoronavirus* subgroup C | | | | | | | | | |
| Ty-BatCoV HKU4 | 30,286 | 0.38 | 52.3 | 67.9 | 67.4 | | 33.8 | 42.6 | 33.4 |
| Pi-BatCoV HKU5 | 30,488 | 0.43 | 53.6 | 68.0 | 67.2 | | 31.4 | 42.2 | 34.7 |
| *Betacoronavirus* subgroup D | | | | | | | | | |
| Ro-BatCoV HKU9 | 29,114 | 0.41 | 48.0 | 66.0 | 68.2 | | 29.3 | 42.5 | 32.4 |
| *Gammacoronavirus* | | | | | | | | | |
| IBV | 27,608 | 0.38 | 41.3 | 60.5 | 60.7 | | 26.1 | 33.3 | 27.9 |
| TCoV | 27,657 | 0.38 | 40.3 | 60.0 | 60.2 | | 26.8 | 32.9 | 26.5 |
| SW1 | 31,686 | 0.39 | 45.0 | 59.8 | 57.9 | | 25.0 | 25.7 | 29.6 |
| *Deltacoronavirus* | | | | | | | | | |
| BuCoV HKU11 | 26,524 | 0.39 | 37.2 | 51.1 | 49.3 | | 26.3 | 28.9 | 23.4 |
| ThCoV HKU12 | 26,425 | 0.38 | 36.9 | 50.8 | 49.0 | | 25.6 | 30.8 | 21.0 |
| MunCoV HKU13 | 26,581 | 0.43 | 36.5 | 51.8 | 50.9 | | 26.5 | 29.3 | 22.0 |

[a] HCoV 229E, human coronavirus 229E; PEDV, porcine epidemic diarrhea virus; TGEV, porcine transmissible gastroenteritis virus; HCoV NL63, human coronavirus NL63; FIPV, feline infectious peritonitis virus; Rh-batCoV HKU2, *Rhinolophus* bat coronavirus HKU2; Mi-BatCoV-1A, *Miniopterus* bat coronavirus 1A; Mi-BatCoV-1B, *Miniopterus* bat coronavirus 1B; Mi-BatCoV HKU8, *Miniopterus* bat coronavirus HKU8; HCoV HKU1, human coronavirus HKU1; HCoV OC43, human coronavirus OC43; MHV, murine hepatitis virus; BCoV, bovine coronavirus; ECoV, equine coronavirus; PHEV, porcine hemagglutinating encephalomyelitis virus; SARS-CoV, SARS coronavirus; SARSr-Rh-batCoV HKU3, SARS-related *Rhinolophus* bat coronavirus HKU3; Ty-BatCoV HKU4, *Tylonycteris* bat coronavirus HKU4; Pi-batCoV HKU5, *Pipistrellus* bat coronavirus HKU5; Ro-batCoV HKU9, *Rousettus* bat coronavirus HKU9; IBV, infectious bronchitis virus; TCoV, turkey coronavirus; BuCoV HKU11, bulbul coronavirus HKU11; ThCoV HKU12, thrush coronavirus HKU12; MunCoV HKU13, munia coronavirus HKU13; SW1, beluga whale coronavirus.

especially in developing countries. In fact, since the 1970s, governments and world food organizations have been promoting rabbit farming in Africa, Asia, and South America, because of the relatively less space and low starting cost required and high breeding rate compared to those of traditional livestock. Rabbits are also commonly kept as pets in domestic households. Further studies, including animal challenge experiments, are needed to understand the pathogenicity and emerging potential of this novel CoV.

Recombination is likely an important event during the evolution of RbCoV HKU14 and members of *Betacoronavirus 1*. CoVs are known to have a high frequency of recombination, which may help them adapt to new hosts. Such recombination has been described for various animal CoVs, including SARSr-Rh-BatCoV and other bat CoVs, MHV, BCoV, infectious bronchitis virus, feline CoV, and canine CoV (17, 22, 23, 27, 32, 33, 52). Natural recombination leading to the generation of different genotypes in HCoV HKU1 has also been described (67, 68). We have also recently found natural recombination among different genotypes of

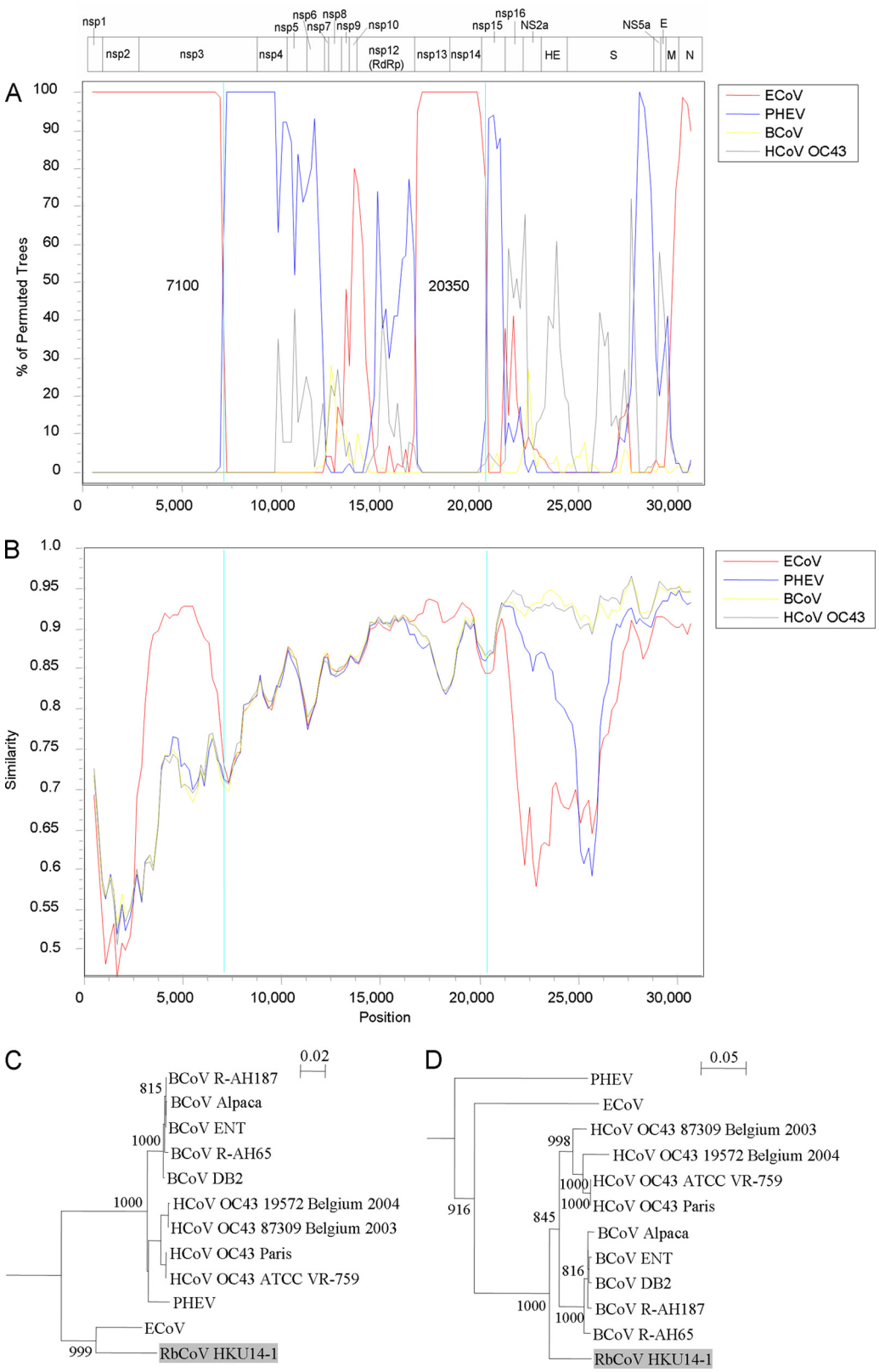


**FIG 6** Recombination analysis of genomes of RbCoV HKU14, BCoV, PHEV, ECoV, and HCoV OC43. (A and B) Bootscanning (A) and similarity plot (B) analyses were conducted with Simplot, version 3.5.1 (F84 model; window size, 1,000 bp; step, 200 bp) on a gapless nucleotide alignment generated with ClustalX, with the genome sequence of strain RbCoV HKU14-1 as the query sequence. (C and D) Phylogenetic analysis of sequences from representative regions corresponding to positions 18033 to 18766 (C) and 25074 to 25908 (D) of RbCoV HKU14-1, showing a shift in phylogenetic clustering upstream and downstream of the potential recombination site at position 20350, respectively. Phylogenetic trees were constructed by the neighbor-joining method using Kimura's two-parameter correction, and bootstrap values were calculated from 1,000 trees. The scale bars indicate the estimated number of substitutions per 50 or 20 amino acids.

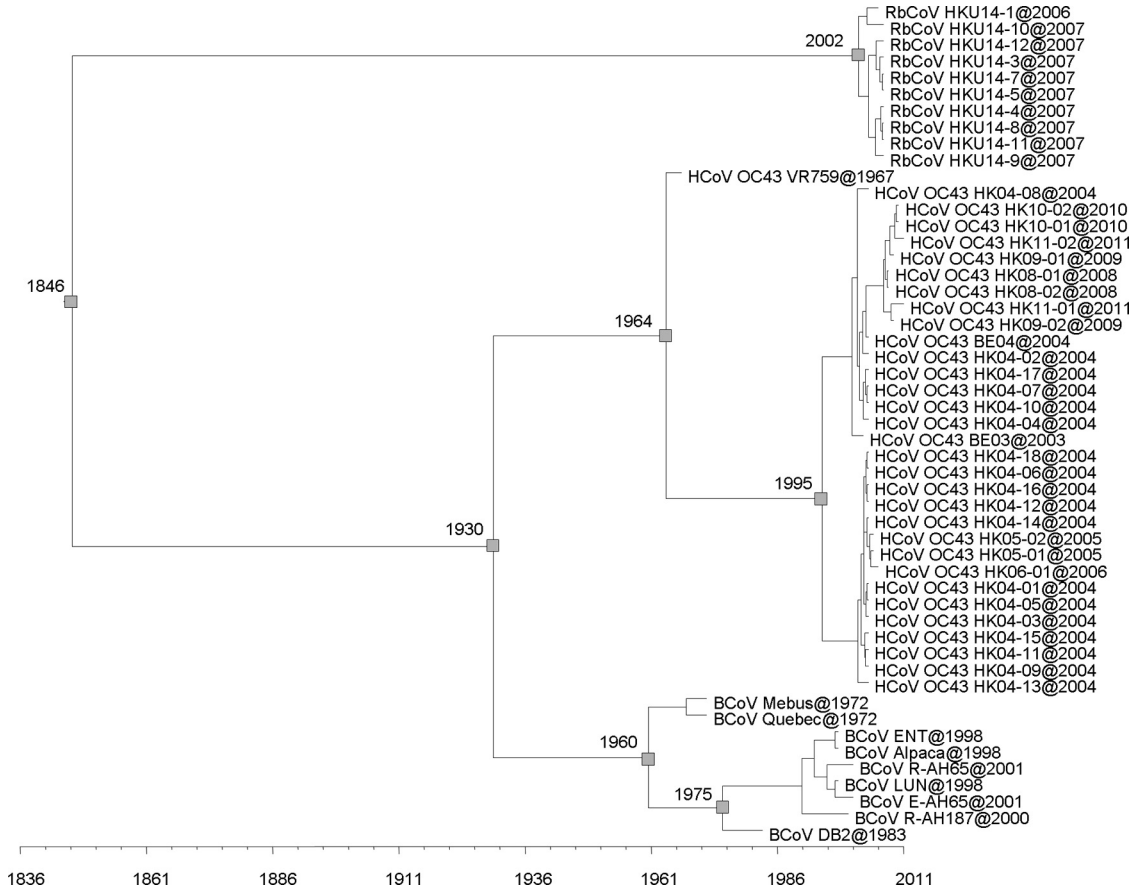


**FIG 7** Estimation of tMRCA of RbCoV HKU14 strains, BCoV/HCoV OC43, and RbCoV HKU14/BCoV/HCoV OC43 based on the RdRp gene. The mean estimated dates are labeled and are represented by gray squares. The taxa are labeled with their sampling dates.

HCoV OC43, giving rise to an emerging genotype D, associated with pneumonia (31). PHEV, BCoV, and HCoV OC43 are genetically and antigenically related betacoronaviruses that have been shown to have originated from a relatively recent common ancestor dating back to the end of the 19th century to the beginning of the 20th century, which is also supported by the present data (Fig. 7) (61, 62). CoVs closely related to BCoV were recently isolated from a sable antelope and a giraffe during an outbreak of winter dysentery in an Ohio wild-animal habitat (1, 16). These CoVs were so closely related to BCoV that no specific genomic markers can allow discrimination between them (1), suggesting that they could well represent spillovers of BCoV to other mammalian hosts. The present study demonstrated recombination events during the evolution of RbCoV HKU14 and members of *Betacoronavirus 1*, which may have arisen during cross-species transmission. However, it remains to be determined if such recombination would have resulted in animal-to-human transmission and the emergence of HCoV OC43. Interestingly, the tMRCA of RbCoV HKU14 was estimated to be rather recent, at around 2002 (HPDs, 1997 to 2005). We speculate that this virus may have emerged as a result of interspecies transmission during the mixing of game food animals in markets during a period of economic boost in China, as in the case of SARS-CoV. Further studies are required to understand the possible existence and prevalence of RbCoV HKU14 in rabbits from other geographical regions. Continuous surveillance studies will also be important to monitor the genetic evolution of CoVs in various food animals.

## ACKNOWLEDGMENTS

We are grateful to the generous support of Carol Yu, Richard Yu, Hui Hoy, and Hui Ming in the genomic sequencing platform.

This work is partly supported by a Research Grant Council grant, University Grant Council; Committee for Research and Conference Grant, Strategic Research Theme Fund, and University Development Fund, The University of Hong Kong; the Hong Kong Special Administrative Region Research Fund for the Control of Infectious Diseases of the Health, Welfare, and Food Bureau; the Providence Foundation Limited, in memory of the late Lui Hac Minh; and the Consultancy Service for Enhancing Laboratory Surveillance of Emerging Infectious Disease for the Hong Kong Special Administrative Region Department of Health.

## REFERENCES

1. **Alekseev KP, et al.** 2008. Bovine-like coronaviruses isolated from four species of captive wild ruminants are homologous to bovine coronaviruses, based on complete genomic sequences. J. Virol. **82**:12422–12431.
2. **Alexander LK, Small JD, Edwards S, Baric RS.** 1992. An experimental model for dilated cardiomyopathy after rabbit coronavirus infection. J. Infect. Dis. **166**:978–985.
3. **Apweiler R, et al.** 2001. The InterPro database, an integrated documentation resource for protein families, domains and functional sites. Nucleic Acids Res. **29**:37–40.
4. **Bateman A, et al.** 2002. The Pfam protein families database. Nucleic Acids Res. **30**:276–280.

5. **Brian DA, Baric RS.** 2005. Coronavirus genome structure and replication. Curr. Top. Microbiol. Immunol. **287**:1–30.
6. **Chouljenko VN, Kousoulas KG, Lin X, Storz J.** 1998. Nucleotide and predicted amino acid sequences of all genes encoded by the 3′ genomic portion (9.5 kb) of respiratory bovine coronaviruses and comparisons among respiratory and enteric coronaviruses. Virus Genes **17**:33–42.
7. **de Groot RJ, et al.** 2011. *Coronaviridae*, p 806–828. *In* King AMQ, Adams MJ, Carstens EB, Lefkowitz, EJ (ed), Virus taxonomy: classification and nomenclature of viruses. Ninth Report of the International Committee on Taxonomy of Viruses, International Union of Microbiological Societies, Virology Division. Elsevier Academic Press, San Diego, CA.
8. **de Haan CA, Masters PS, Shen X, Weiss S, Rottier PJ.** 2002. The group-specific murine coronavirus genes are not essential, but their deletion, by reverse genetics, is attenuating in the natural host. Virology **296**: 177–189.
9. **Dominguez SR, O'Shea TJ, Oko LM, Holmes KV.** 2007. Detection of group 1 coronaviruses in bats in North America. Emerg. Infect. Dis. **13**: 1295–1300.
10. **Dong BQ, et al.** 2007. Detection of a novel and highly divergent coronavirus from Asian leopard cats and Chinese ferret badgers in Southern China. J. Virol. **81**:6920–6926.
11. **Drummond AJ, Rambaut A.** 2007. BEAST: Bayesian evolutionary analysis by sampling trees. BMC Evol. Biol. **7**:214.
12. **Fouchier RA, et al.** 2004. A previously undescribed coronavirus associated with respiratory disease in humans. Proc. Natl. Acad. Sci. U. S. A. **101**:6212–6216.
13. **Gloza-Rausch F, et al.** 2008. Detection and prevalence patterns of group I coronaviruses in bats, northern Germany. Emerg. Infect. Dis. **14**:626–631.
14. **Goebel SJ, Hsue B, Dombrowski TF, Masters PS.** 2004. Characterization of the RNA components of a putative molecular switch in the 3′ untranslated region of the murine coronavirus genome. J. Virol. **78**:669–682.
15. **Guan Y, et al.** 2003. Isolation and characterization of viruses related to the SARS coronavirus from animals in southern China. Science **302**:276–278.
16. **Hasoksuz M, et al.** 2007. Biologic, antigenic, and full-length genomic characterization of a bovine-like coronavirus isolated from a giraffe. J. Virol. **81**:4981–4990.
17. **Herrewegh AA, Smeenk I, Horzinek MC, Rottier PJ, de Groot RJ.** 1998. Feline coronavirus type II strains 79-1683 and 79-1146 originate from a double recombination between feline coronavirus type I and canine coronavirus. J. Virol. **72**:4508–4514.
18. **Hofmann KS.** 1993. TMbase—a database of membrane spanning proteins segments. Biol. Chem. Hoppe Seyler **374**:166.
19. **Huang Y, Lau SK, Woo PC, Yuen KY.** 2008. CoVDB: a comprehensive database for comparative analysis of coronavirus genes and genomes. Nucleic Acids Res. **36**:D504–D511.
20. **Jeong YS, Repass JF, Kim YN, Hwang SM, Makino S.** 1996. Coronavirus transcription mediated by sequences flanking the transcription consensus sequence. Virology **217**:311–322.
21. **Jonassen CM, et al.** 2005. Molecular identification and characterization of novel coronaviruses infecting graylag geese (*Anser anser*), feral pigeons (*Columbia livia*) and mallards (*Anas platyrhynchos*). J. Gen. Virol. **86**: 1597–1607.
22. **Keck JG, et al.** 1988. In vivo RNA-RNA recombination of coronavirus in mouse brain. J. Virol. **62**:1810–1813.
23. **Kottier SA, Cavanagh D, Britton P.** 1995. Experimental evidence of recombination in coronavirus infectious bronchitis virus. Virology **213**: 569–580.
24. **Kuiken T, et al.** 2003. Newly discovered coronavirus as the primary cause of severe acute respiratory syndrome. Lancet **362**:263–270.
25. **Lai MM, Cavanagh D.** 1997. The molecular biology of coronaviruses. Adv. Virus Res. **48**:1–100.
26. **Lau SK, et al.** 2009. Confirmation of the first Hong Kong case of human infection by novel swine-origin influenza A (H1N1) virus diagnosed using ultrarapid, real-time reverse transcriptase PCR. J. Clin. Microbiol. **47**: 2344–2346.
27. **Lau SK, et al.** 2010. Ecoepidemiology and complete genome comparison of different strains of severe acute respiratory syndrome-related Rhinolophus bat coronavirus in China reveal bats as a reservoir for acute, self-limiting infection that allows recombination events. J. Virol. **84**:2808–2819.
28. **Lau SK, et al.** 2006. Coronavirus HKU1 and other coronavirus infections in Hong Kong. J. Clin. Microbiol. **44**:2063–2071.
29. **Lau SK, et al.** 2005. Severe acute respiratory syndrome coronavirus-like virus in Chinese horseshoe bats. Proc. Natl. Acad. Sci. U. S. A. **102**:14040–14045.
30. **Lau SK, et al.** 2007. Complete genome sequence of bat coronavirus HKU2 from Chinese horseshoe bats revealed a much smaller spike gene with a different evolutionary lineage from the rest of the genome. Virology **367**: 428–439.
31. **Lau SK, et al.** 2011. Molecular epidemiology of human coronavirus OC43 reveals evolution of different genotypes over time and recent emergence of a novel genotype due to natural recombination. J. Virol. **85**:11325–11337.
32. **Lau SK, et al.** 2010. Coexistence of different genotypes in the same bat and serological characterization of Rousettus bat coronavirus HKU9 belonging to a novel *Betacoronavirus* subgroup. J. Virol. **84**:11385–11394.
33. **Lavi E, Haluskey JA, Masters PS.** 1998. The pathogenesis of MHV nucleocapsid gene chimeric viruses. Adv. Exp. Med. Biol. **440**:537–541.
34. **Li IW, et al.** 2009. Differential susceptibility of different cell lines to swine-origin influenza A H1N1, seasonal human influenza A H1N1, and avian influenza A H5N1 viruses. J. Clin. Virol. **46**:325–330.
35. **Li W, et al.** 2005. Bats are natural reservoirs of SARS-like coronaviruses. Science **310**:676–679.
36. **Marra MA, et al.** 2003. The genome sequence of the SARS-associated coronavirus. Science **300**:1399–1404.
37. **Mihindukulasuriya KA, Wu G, St Leger J, Nordhausen RW, Wang D.** 2008. Identification of a novel coronavirus from a beluga whale by using a panviral microarray. J. Virol. **82**:5084–5088.
38. **Netland J, et al.** 2007. Enhancement of murine coronavirus replication by severe acute respiratory syndrome coronavirus protein 6 requires the N-terminal hydrophobic region but not C-terminal sorting motifs. J. Virol. **81**:11520–11525.
39. **Nowak R.** 1999. Walker's mammals of the world, 6th ed. Johns Hopkins University Press, Baltimore, MD.
40. **Pall GS, Hamilton AJ.** 2008. Improved Northern blot method for enhanced detection of small RNA. Nat. Protoc. **3**:1077–1084.
41. **Parker SE, Gallagher TM, Buchmeier MJ.** 1989. Sequence analysis reveals extensive polymorphism and evidence of deletions within the E2 glycoprotein gene of several strains of murine hepatitis virus. Virology **173**: 664–673.
42. **Peiris JS, et al.** 2003. Coronavirus as a possible cause of severe acute respiratory syndrome. Lancet **361**:1319–1325.
43. **Poon LL, et al.** 2005. Identification of a novel coronavirus in bats. J. Virol. **79**:2001–2009.
44. **Prabakaran P, et al.** 2006. Structure of severe acute respiratory syndrome coronavirus receptor-binding domain complexed with neutralizing antibody. J. Biol. Chem. **281**:15829–15836.
45. **Pyrc K, Jebbink MF, Berkhout B, van der Hoek L.** 2004. Genome structure and transcriptional regulation of human coronavirus NL63. Virol. J. **1**:7.
46. **Rota PA, et al.** 2003. Characterization of a novel coronavirus associated with severe acute respiratory syndrome. Science **300**:1394–1399.
47. **Sawicki SG, Sawicki DL, Siddell SG.** 2007. A contemporary view of coronavirus transcription. J. Virol. **81**:20–29.
48. **Schaad MC, Chen W, Peel SA, Baric RS.** 1993. Studies into the mechanism for MHV transcription. Adv. Exp. Med. Biol. **342**:85–90.
49. **Schultze B, Herrler G.** 1992. Bovine coronavirus uses N-acetyl-9-O-acetylneuraminic acid as a receptor determinant to initiate the infection of cultured cells. J. Gen. Virol. **73**:901–906.
50. **Schwarz B, Routledge E, Siddell SG.** 1990. Murine coronavirus nonstructural protein ns2 is not essential for virus replication in transformed cells. J. Virol. **64**:4784–4791.
51. **Small JD, Woods RD.** 1987. Relatedness of rabbit coronavirus to other coronaviruses. Adv. Exp. Med. Biol. **218**:521–527.
52. **Smits SL, et al.** 2005. Nidovirus sialate-O-acetylesterases: evolution and substrate specificity of coronaviral and toroviral receptor-destroying enzymes. J. Biol. Chem. **280**:6933–6941.
53. **Snijder EJ, et al.** 2003. Unique and conserved features of genome and proteome of SARS-coronavirus, an early split-off from the coronavirus group 2 lineage. J. Mol. Biol. **331**:991–1004.
54. **Sonnhammer EL, von Heijne G, Krogh A.** 1998. A hidden Markov model for predicting transmembrane helices in protein sequences. Proc. Int. Conf. Intell. Syst. Mol. Biol. **6**:175–182.
55. **Suchard MA, Weiss RE, Sinsheimer JS.** 2001. Bayesian selection of continuous-time Markov chain evolutionary models. Mol. Biol. Evol. **18**: 1001–1013.

56. **Tamura K, Dudley J, Nei M, Kumar S.** 2007. MEGA4: Molecular Evolutionary Genetics Analysis (MEGA) software version 4.0. Mol. Biol. Evol. **24**:1596–1599.
57. **Tang XC, et al.** 2006. Prevalence and genetic diversity of coronaviruses in bats from China. J. Virol. **80**:7481–7490.
58. **Thiel V, Siddell SG.** 1994. Internal ribosome entry in the coding region of murine hepatitis virus mRNA 5. J. Gen. Virol. **75**:3041–3046.
59. **Tong S, et al.** 2009. Detection of novel SARS-like and other coronaviruses in bats from Kenya. Emerg. Infect. Dis. **15**:482–485.
60. **van der Hoek L, et al.** 2004. Identification of a new human coronavirus. Nat. Med. **10**:368–373.
61. **Vijgen L, et al.** 2005. Complete genomic sequence of human coronavirus OC43: molecular clock analysis suggests a relatively recent zoonotic coronavirus transmission event. J. Virol. **79**:1595–1604.
62. **Vijgen L, et al.** 2006. Evolutionary history of the closely related group 2 coronaviruses: porcine hemagglutinating encephalomyelitis virus, bovine coronavirus, and human coronavirus OC43. J. Virol. **80**:7270–7274.
63. **Vlasak R, Luytjes W, Spaan W, Palese P.** 1988. Human and bovine coronaviruses recognize sialic acid-containing receptors similar to those of influenza C viruses. Proc. Natl. Acad. Sci. U. S. A. **85**:4526–4529.
64. **Woo PC, et al.** 2007. Comparative analysis of twelve genomes of three novel group 2c and group 2d coronaviruses reveals unique group and subgroup features. J. Virol. **81**:1574–1585.
65. **Woo PC, Lau SK, Yuen KY.** 2006. Infectious diseases emerging from Chinese wet-markets: zoonotic origins of severe respiratory viral infections. Curr. Opin. Infect. Dis. **19**:401–407.
66. **Woo PC, et al.** 2004. False positive results in a recombinant severe acute respiratory syndrome-associated coronavirus (SARS-CoV) nucleocapsid enzyme-linked immunosorbent assay due to HCoV-OC43 and HCoV-229E rectified by Western blotting with recombinant SARS-CoV spike polyprotein. J. Clin. Microbiol. **42**:5885–5888.
67. **Woo PC, et al.** 2006. Comparative analysis of 22 coronavirus HKU1 genomes reveals a novel genotype and evidence of natural recombination in coronavirus HKU1. J. Virol. **80**:7136–7145.
68. **Woo PC, et al.** 2005. Characterization and complete genome sequence of a novel coronavirus, coronavirus HKU1, from patients with pneumonia. J. Virol. **79**:884–895.
69. **Woo PC, et al.** 25 January 2012. Discovery of seven novel mammalian and avian coronaviruses in Deltacoronavirus supports bat coronaviruses as the gene source of Alphacoronavirus and Betacoronavirus and avian coronaviruses as the gene source of Gammacoronavirus and Deltacoronavirus. J. Virol. doi:10.1128/JVI.06540-11.
70. **Woo PC, et al.** 2009. Comparative analysis of complete genome sequences of three avian coronaviruses reveals a novel group 3c coronavirus. J. Virol. **83**:908–917.
71. **Woo PC, et al.** 2004. Relative rates of non-pneumonic SARS coronavirus infection and SARS coronavirus pneumonia. Lancet **363**:841–845.
72. **Woo PC, et al.** 2005. Clinical and molecular epidemiological features of coronavirus HKU1-associated community-acquired pneumonia. J. Infect. Dis. **192**:1898–1907.
73. **Woo PC, et al.** 2006. Molecular diversity of coronaviruses in bats. Virology **351**:180–187.
74. **Woo PC, Lau SK, Huang Y, Yuen KY.** 2009. Coronavirus diversity, phylogeny and interspecies jumping. Exp. Biol. Med. (Maywood) **234**:1117–1127.
75. **Wu HY, Ozdarendeli A, Brian DA.** 2006. Bovine coronavirus 5′-proximal genomic acceptor hotspot for discontinuous transcription is 65 nucleotides wide. J. Virol. **80**:2183–2193.
76. **Yoo D, Deregt D.** 2001. A single amino acid change within antigenic domain II of the spike protein of bovine coronavirus confers resistance to virus neutralization. Clin. Diagn. Lab. Immunol. **8**:297–302.
77. **Zhang J, et al.** 2007. Genomic characterization of equine coronavirus. Virology **369**:92–104.
78. **Zhang XM, Kousoulas KG, Storz J.** 1991. The hemagglutinin/esterase glycoprotein of bovine coronaviruses: sequence and functional comparisons between virulent and avirulent strains. Virology **185**:847–852.
79. **Ziebuhr J, Thiel V, Gorbalenya AE.** 2001. The autocatalytic release of a putative RNA virus transcription factor from its polyprotein precursor involves two paralogous papain-like proteases that cleave the same peptide bond. J. Biol. Chem. **276**:33220–33232.